

Random magnetic anisotropy in a new compound Sm_2AgSi_3

Baidyanath Sahu,^{1, a)} R. Djoumessi Fobasso,¹ and André M. Strydom¹

Highly Correlated Matter Research Group, Department of Physics, University of Johannesburg, PO Box 524, Auckland Park 2006, South Africa

We report the experimental study on the structural and magnetic properties of a new ternary intermetallic compound Sm_2AgSi_3 . The properties of the sample were investigated in detail by X-ray diffraction, dc-magnetization, and heat capacity measurements. The polycrystalline compound of Sm_2AgSi_3 crystallizes in the ThSi_2 -type tetragonal structure (space group I_{41}/amd). The temperature-dependent dc-magnetization and heat capacity results demonstrate that the compound undergoes ferromagnetic behaviour with a Curie temperature (T_C) of 14 K. The large coercive field in hysteresis loops and the thermomagnetic irreversibility in the ferromagnetic region revealed that the compound exhibits a large magnetic anisotropy. The magnitude of the applied field and the coercivity obtained from the M-H loops corroborate with the thermomagnetic irreversibility in the magnetization data. The magnetic contribution of the heat capacity reveals a broad Schottky-type anomaly above T_C , due to the presence of the crystal electric field effect of Sm^{3+} in Sm_2AgSi_3 .

Keywords: Ferromagnet; Magnetic anisotropy; Thermomagnetic irreversibility; Schottky peak.

The ternary intermetallic compounds R_2TX_3 (R = rare earths, T = transition metals, X = Si, Ge, Al, and In), are extensively studied for their structural and magnetic properties. Most of the compounds with R_2TX_3 stoichiometry form in ThSi_2 type both hexagonal and tetragonal crystal structure. The magnetic R ions occupy the Th position, while the T and X ions mutually occupy the Si positions in ThSi_2 ¹⁻³. Recently, the random magnetic anisotropy in a polycrystalline ThSi_2 type hexagonal compound Sm_2NiSi_3 was confirmed from the temperature dependence of zero-field cooled (ZFC) and field-cooled (FC) magnetization and magnetic entropy changes^{4,5}.

Samarium (Sm) based intermetallic compounds have gained considerable interest because of their interesting properties such as superconductivity, magneto-resistance, magnetic and non magnetic behaviour⁶⁻⁸. Sm based ternary and binary compounds can show large magnetic hysteresis due to their large magnetic anisotropy and may be used as a permanent magnet^{9,10}. A strong magneto-crystalline anisotropy may be produced by Sm^{3+} ion as a consequence of the crystal electric field (CEF) effect acting on the 4f-electrons.

In recent years, the development of magnetic materials has posed a great challenge to researchers. To the best of our knowledge, the existence of Sm_2AgSi_3 compound was not earlier reported. In this work, we have reported the detailed synthesis process and magnetic properties of a new compound Sm_2AgSi_3 . The large random magnetic anisotropy in Sm_2AgSi_3 is also demonstrated.

A. Experimental Set-up

A polycrystalline sample Sm_2AgSi_3 was prepared under ultra-high purity argon atmosphere using the stan-

dard arc-melting technique. The melted ingot was turned over and remelted five times to ensure a good homogeneity. The melted sample was wrapped in a tantalum foil and sealed in a vacuum quartz tube. The tube was kept in a furnace for annealing at 1373 K for one week and then quenched in cold water. The sample was characterized by powder X-ray diffraction (XRD) using CuK_α radiation of a Rigaku XRD machine. The Rietveld analysis of XRD patterns was carried out using FULLPROF software^{11,12}. The temperature and field dependence of dc-magnetization measurement was performed using a Dynacool physical properties measurement system (PPMS) made by Quantum Design, USA. Heat capacity measurements were carried out using the same equipment.

B. Results and Discussion

1. X-ray Diffraction

Fig. 1 shows the room-temperature powder XRD pattern along with the Rietveld refinement fitting profile of polycrystalline Sm_2AgSi_3 . The Rietveld refinement result reveals that the compound form in a β - ThSi_2 -type of tetragonal structure with space group I_{41}/amd . The crystallographic parameters from the refinement are listed in Table I. The inset of Fig. 1 shows the schematic diagram of the crystal structure of Sm_2AgSi_3 . The shortest distance between Sm atoms is 4.119 Å, and is twice larger than the expected ionic radius of Sm^{3+} ($r_{\text{Sm}} = 0.958$ Å). This suggests that there is a weak interaction between the rare-earth atoms in Sm_2AgSi_3 .

2. Magnetic Properties

Fig. 2 shows the temperature dependence of ZFC and FC dc-magnetic susceptibility ($\chi(T)$) with an applied field (H_{app}) of 1 T. The dc- $\chi(T)$ shows a typical para-

^{a)}Electronic mail: baidyanathsahu@gmail.com

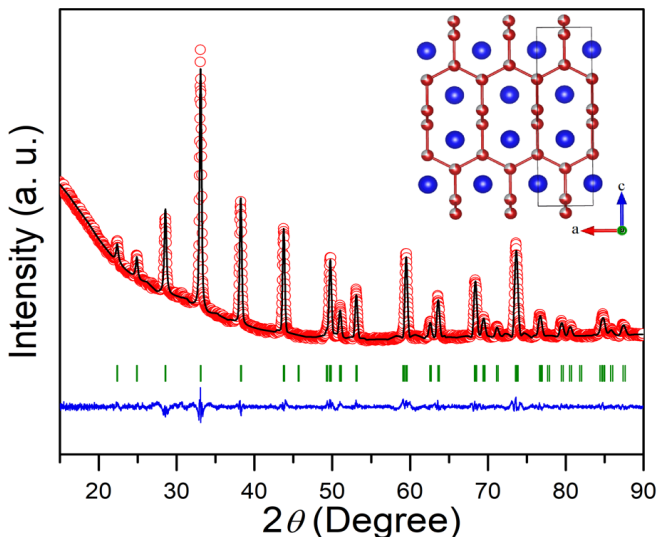


FIG. 1. X-ray powder diffraction data for Sm_2AgSi_3 . Red symbols represent the experimental data and the black line represents the calculated data. The difference between experimental and calculated data is shown as a blue line. A set of vertical bars represents the Bragg peak positions of the tetragonal α - ThSi_2 type structure. Inset: The schematic representation of the tetragonal crystal structure of Sm_2AgSi_3 . The blue balls are for Sm and silver-red color balls are for Ag+Si.

TABLE I. The lattice parameters, unit cell volume and the atomic coordinate positions of Sm_2AgSi_3 obtained from the Rietveld refinement of XRD patterns. The refinement quality parameter is $\chi^2 = 5.7$.

| a = b | | 4.128(2) Å | | |
|---|---------|---------------------------|-----|-----------|
| c | | 14.254(2) Å | | |
| V | | 242.890(1) Å ³ | | |
| Atomic coordinates for Sm_2AgSi_3 | | | | |
| Atom | Wyckoff | x | y | z |
| Sm | 4a | 0 | 3/4 | 1/8 |
| Ag | 8e | 0 | 1/4 | 0.2895(2) |
| Si | 8e | 0 | 1/4 | 0.2895(2) |

magnetic to ferromagnetic transition in this compound. The Curie temperature (T_C) was found to be 14 K from the peak of the $d\chi(T)/dT$ curve. The inverse dc-magnetic susceptibility (not shown in figure) does not follow the Curie-Weiss relation. Hence, the modified Curie-Weiss law, $\chi = [C/(T-\theta_P)] + \chi_0$, (where C is the Curie constant, θ_P is the Weiss paramagnetic temperature and χ_0 is the temperature-independent magnetic susceptibility which includes the core-electron diamagnetism) was fitted on the $\chi(T)$ of Fig. 2 for $T > 20$ K. The least-squares fit (LSQ) fit to the experimental data yielded $\theta_P = 12$ K and $\chi_0 = 3.1 \times 10^{-4}$ emu/mole.Oe. The positive value of θ_P shows that the dominant inter-

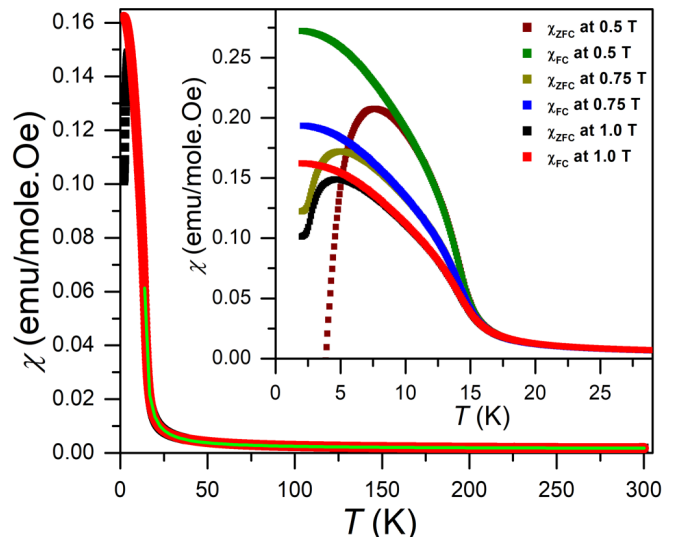


FIG. 2. Temperature dependence of the field-cooled (FC) and zero-field-cooled (ZFC) dc-magnetic susceptibility ($\chi(T)$) at 1 T of Sm_2AgSi_3 along with a fit to the data (green line) of a modified Curie-Weiss law. Inset shows ZFC and FC of $\chi(T)$ at low temperature region for various applied magnetic fields.

action is ferromagnetic in Sm_2AgSi_3 . The effective magnetic moment (μ_{eff}) value was calculated from the fitting parameter value of C and found to be $0.57 \mu_B/\text{Sm}^{3+}$. A small deviation of μ_{eff} from the theoretical value of free ion Sm^{3+} [$g\sqrt{J(J+1)} = 0.85 \mu_B$] may arise from crystal field effects (CEF). The expanded region in low temperature of $\chi(T)$ for different magnetic fields shows in the inset of Fig. 2. As seen in the inset, there is a thermal magnetic irreversibility (TMI) shown between the data collected in the ZFC and FC protocols. The TMI point is defined as the temperature at which the χ_{ZFC} and χ_{FC} curves bifurcate from each other. It is also observed that TMI depends on the H_{app} . It can be believed that the large magnetic anisotropy may cause the TMI behavior in $\chi(T)$ for high $H_{app} = 1.0$ T.

Fig. 3 shows the field-dependent magnetization $M(H)$ loops at different temperatures. The well-defined hysteresis below T_C is observed in the ferromagnetic ordered region of Sm_2AgSi_3 . The $M(H)$ loops do not saturate even at a high field value of 9 T at 2 K. The spontaneous magnetization was calculated from $M(H)$ at 2 K, and the obtained value is $0.25 \mu_B/\text{Sm}$. This value is smaller by a considerable margin than the expected saturation moment value for parallel alignment of Sm^{3+} spin ($gJ = 0.71 \mu_B$, with $g = 2/7$, and $J = 5/2$). The low magnetization value is attributed to the influence of the magnetic anisotropy in saturation. As seen in the M-H loops, a large value of coercivity (H_C) of 0.8 T at 2 K appears for a polycrystalline rare-earth based compound. This large H_C may result from the random magnetic anisotropy of the sample. For more details, the $M(H)$ loops were measured at different temperatures. The $H_C(T)$ and remanence magnetization was estimated from $M(H)$ loops

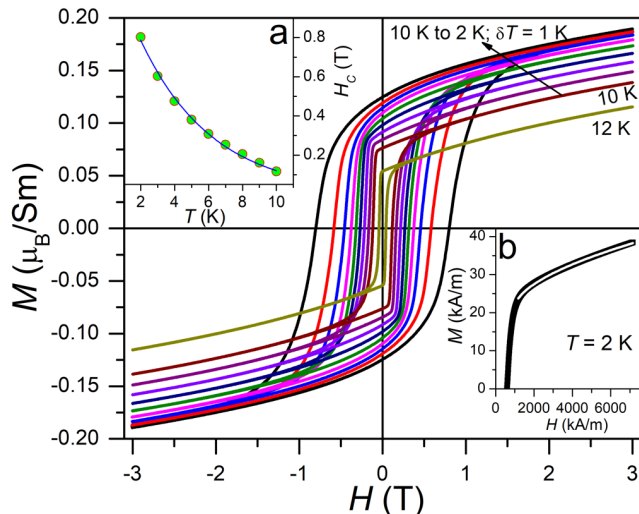


FIG. 3. Hysteresis loops of Sm_2AgSi_3 for different temperatures between 2 and 12 K. Inset (a): the temperatures dependence of the coercivity along with the fitting line explained in the text. Inset (b): the high field magnetization data with the fitted line by using Eq. 1.

for each temperature and found to gradually decrease with increasing temperature. The temperature variation $H_C(T)$ is plotted in inset (a) of Fig. 3. An exponential behavior described by the relation $H_C(T) = A \exp(-BT)$ is observed¹³. The fitting is shown as a blue line on the data. The best fitting parameters obtained from the $H_C(T)$ vs. T curve are $A = 1.256$ T and $B = 0.234$ K^{-1} represent the H_C at 0 K and the steep temperature dependence of $H_C(T)$ in ferromagnet suggests that the observed hysteresis of Sm_2AgSi_3 is appropriate for large magnetic anisotropy.

The magneto-crystalline anisotropy constant of magnetic materials are evaluated from the law of approach to saturation. The law of approach to saturation is therefore applied on the $M(H)$ by fitting Eq. 1 on the high magnetic field magnetization data as¹⁴⁻¹⁶:

$$M = M_S \left[1 - \frac{D}{H^2} \right] + \chi_0 H^{1/2}, \quad (1)$$

where M_S (in A/m) is the saturation magnetization. Here, D is a function of magnetic anisotropy energy and $\chi_0 H^{1/2}$ denotes the term related to para-process. The parameter D is expressed as:

$$D = \frac{8}{105} \frac{K_1^2}{\mu_0^2 M_S^2} (\text{A/m})^2, \quad (2)$$

where K_1 is the anisotropy constant in $\text{J}\cdot\text{m}^{-3}$ and μ_0 is the free space magnetic permeability. For polycrystalline material, it is assumed that the overall possible orientations of the individual crystallites are averaged.

The value of K_1 was estimated by using the fitting parameters B and M_S on Eq. 2. The obtained K_1 value is $|K_1| = 1.3 \times 10^5$ $\text{J}\cdot\text{m}^{-3}$ at 2 K. The obtained value of $|K_1|$ is comparable with 9.2×10^6 $\text{J}\cdot\text{m}^{-3}$ for $\text{SmFe}_{11}\text{Ti}$ and 4.0×10^6 $\text{J}\cdot\text{m}^{-3}$ for $\text{Sm}_3\text{Fe}_5\text{O}_{12}$ ^{17,18}. The observed large hysteresis loop in $M(H)$ and comparable value of $|K_1|$ revealed that a random magnetic anisotropy exists in Sm_2AgSi_3 .

The anisotropy field plays a crucial role in determining the FC magnetic susceptibilities (χ_{FC}) and the ZFC magnetic susceptibilities (χ_{ZFC}) at a given field value. The temperature variation of anisotropy field and H_{app} for measuring $\chi(T)$ plays a major role in determining the degree of TMI¹⁹. Joy *et al.*,^{19,20} have proposed an empirical relation between H_{app} , H_C , χ_{FC} and χ_{ZFC} for a ferromagnetic system:

$$\chi_{ZFC} = \chi_{FC} \frac{H_{app}}{H_{app} + H_C}, \quad (3)$$

This Eq. 3 indicates that the χ_{ZFC} and χ_{FC} should overlap in that temperature regime for $H_{app} \gg H_C$. However, the difference between the χ_{ZFC} and χ_{FC} values is large for $H_{app} \ll H_C$. Hence, it can be assume that the hysteresis between χ_{ZFC} and χ_{FC} arises even at high field H_{app} of 1.0 T due to the magnetic anisotropy in the sample. However, the χ_{ZFC} for $H = 0.5$ T starting from negative values of at low temperatures is due to this anisotropic sample being cooled in a net negative trapping field. This trap magnetic field commonly exists in the PPMS superconducting solenoid magnet²¹.

3. Heat Capacity

The temperature variation of heat capacity ($C_p(T)$) of Sm_2AgSi_3 and of the isostructural non-magnetic compound La_2AgSi_3 are depicted in Fig. 4. A value of 147 J/(mol.-K) is attained at 300 K, very closed to the Dulong-Petit limit $3nR = 149.65$ J/(mol.-K) ($n = 6$ is the number of atoms per formula unit, R stands for the gas constant). At low temperatures, $C_p(T)$ exhibits an anomaly in Sm_2AgSi_3 for the characteristic of a magnetic phase transition. The transition temperature of ~ 13 K is defined from the peak of $C_p(T)$, and is consistent with the $M(T)$ data.

The magnetic contribution of heat capacity (C_{4f}) for Sm_2AgSi_3 was estimated by subtracting the $C_p(T)$ data of La_2AgSi_3 from that of Sm_2AgSi_3 data and is shown in the inset of Fig. 4. As seen in the inset of Fig. 4, $C_{4f}(T)$ exhibits a broad hump above the transition temperature, indicating a Schottky type anomaly caused by crystalline electric field (CEF) present in this compound. The magnetic entropy S_{4f} was estimated using the formula $S_{4f} = \int (C_{4f}/T) dT$. The temperature variation of S_{4f} is shown in the right-hand axis of Fig. 4. The magnetic entropy is very close to $R \ln 2$ at T_C , indicating the

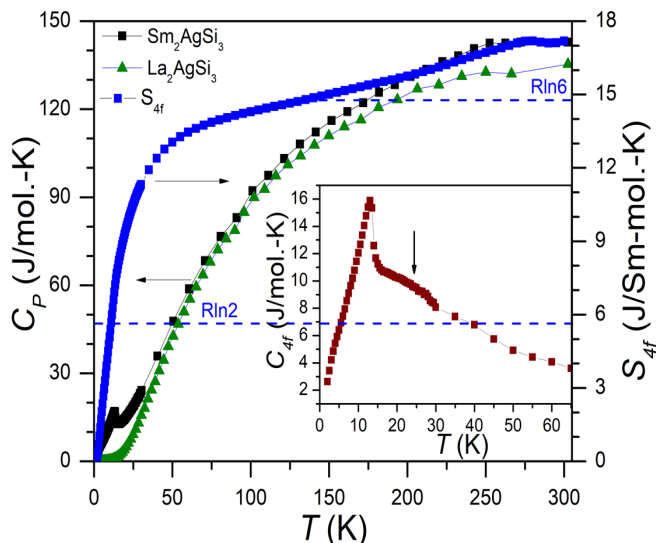


FIG. 4. (Left scale) Temperature dependence of zero field heat capacity (C_P) of La_2AgSi_3 , and Sm_2AgSi_3 . (Right scale) Temperature dependence of magnetic entropy of Sm_2AgSi_3 . Inset: (left with bottom scale) temperature dependence for magnetic contribution of (C_P) for Sm_2AgSi_3 at low temperature region. (left with top scale) $T^{3/2}$ dependence of magnetic contribution of heat capacity for Sm_2AgSi_3 .

presence of a doublet ground state in the magnetic system. S_{4f} increases above T_C and displays a tendency to saturate above 50 K. S_{4f} saturates around a value of $R\ln 6$, indicating that the highest excited crystal field level contributes to magnetic entropy.

4. Summary

In this work the Sm_2AgSi_3 compound was synthesized and found to be stoichiometric and crystallizing in the $\beta\text{-ThSi}_2$ -type tetragonal structure. The experimental results indicate that the compound undergoes a paramagnetic to ferromagnetic phase transition at $T_C = 14$ K. The large H_C confirms that the compound possesses a large large anisotropy. The presence of magnetic anisotropy plays a role in the TMI between χ_{ZFC} and χ_{FC} , and are related through H_C . The C_{4f} results indicate that the Schottky type anomaly is present due to the crystalline electric field (CEF), which may result in a large magnetic anisotropy. The present results pave the way for future promising research of magnetic properties in new R_2TX_3 series of compounds.

Acknowledgements

This work is supported by a Global Excellence and Stature (UJ-GES) fellowship, University of Johannesburg, South Africa. DFR thanks OWSD and SIDA for the fellowship towards PhD studies. AMS thanks the URC/FRC and the SA-NRF (93549) for financial support of UJ for assistance of financial support.

References

- ¹Z.Y. Pan, C.D. Cao, X.J. Bai, R.B. Song, J.B. Zheng, and L.B. Duan, Chinese Physics B, **22** (2013) 056102.
- ²V.H. Tran, Journal of Physics: Condensed Matter, **8** (1996) 6267.
- ³S. Sarkar, D. Mumbaraddi, P. Halappa, D. Kalsi, S. Rayaprol, and S. Peter, Journal of Solid State Chemistry, **229** (2015) 287–295.
- ⁴S. Pakhira, A. K. Kundu, C. Mazumdar, and R. Ranganathan, Journal of Physics: Condensed Matter, **30** (2018) 215601.
- ⁵S. Pakhira, C. Mazumdar, R. Ranganathan, and S. Giri, Journal of Alloys and Compounds, **742** (2018): 391–401.
- ⁶G. A. Artioli, F. Hammerath, M. C. Mozzati, P. Carretta, F. Corana, B. Manucci, S. Margadonna, and L. Malavasi, Chemical Communications, **51** (2015) 1092–1095.
- ⁷H. Fujishiro, K. Yokoyama, T. Oka, and K. Noto, Superconductor Science and Technology, **17** (2003) 51.
- ⁸E. V. Sampathkumaran, P. L. Paulose, and R. Mallik, Physical Review B, **54** (1996) R3710.
- ⁹T. Toliński, A. Kowalczyk, A. Szlaferek, B. Andrzejewski, J. Kováč, and M. Timko, Journal of Alloys and Compounds, **347** (2002) 31–35.
- ¹⁰A. E. Ray, Journal of Applied Physics, **55** (1984) 2094–2096.
- ¹¹H. M. Rietveld, Journal of Applied Crystallography, **2** (1969) 65.
- ¹²Rodriguez-Carvajal J., Fullprof Suite <http://www.ill.eu/sites/fullprof/> (2017).
- ¹³M. S. Henriques, D. I. Gorbunov, A. V. Andreev, X. Fabrèges, A. Gukasov, M. Uhlarz, V. Petříček, B. Ouladdiaf, and J. Wosnitza, Physical Review B, **97** (2018) 014431.
- ¹⁴S. Chikazumi, Physics of Ferromagnetism, second ed., Oxford University Press, Oxford, 1997, p.506.
- ¹⁵O. Kohmoto, Journal of Applied Physics, **53** (1982) 7486.
- ¹⁶A. Bhattacharyya, S. Giri, and S. Majumdar, Journal of Magnetism and Magnetic Materials, **323** (2011) 1484–1489.
- ¹⁷H. T. Kim, Y. B. Kim, C. S. Kim, and H. Jin, Journal of Magnetism and Magnetic Materials, **152** (1996) 387–390.
- ¹⁸K. P. Belov, A. K. Gapeev, R. Z. Levitin, A. S. Markosyan, and Yu. F. Popov, Sou. Phys. Journal of Experimental and Theoretical Physics **41** (1975) 117.
- ¹⁹P. A. Joy, PS Anil Kumar, and S. K. Date, Journal of Physics: Condensed Matter, **10** (1998) 11049.
- ²⁰PS Anil Kumar, P. A. Joy, and S. K. Date, Solid State Communications, **108** (1998) 67–70.
- ²¹D. X. Li, A. Dönni, Y. Kimura, Y. Shiokawa, Y. Homma, Y. Haga, E. Yamamoto, T. Honma, and Y. Onuki, Journal of Physics: Condensed Matter, **11** (1999) 8263.